fire

MDPI

Article

Pore-Scale Research on Spontaneous Combustion of Coal Pile Utilizing Lattice Boltzmann Method

Yongyu Wang [1], Man Zhang [1], Xingpeng Wu [1], Dongfeng Zhu [2], Kaihua Lu [1,*], Sheng Xue [3,*] and Junjie Hu [1]

[1] Faculty of Engineering, China University of Geosciences, Wuhan 430074, China
[2] School of Minerals and Energy Resources Engineering, University of New South Wales, Sydney 2052, Australia
[3] Joint National-Local Engineering Research Centre for Safe and Precise Coal Mining, Anhui University of Science and Technology, Huainan 232001, China
* Correspondence: lukh@cug.edu.cn (K.L.); sheng.xue@aust.edu.cn (S.X.)

Abstract

Spontaneous combustion of coal piles threatens the production and transportation safety of coal mining, which is attracting more and more attention. To understand the underlying physics, conducting pore-scale research on the spontaneous combustion of coal piles is critical. To enable pore-scale research, a pore-scale model of the spontaneous combustion of a coal pile is described, and governing equations are introduced. To understand the competition between airflow, heat–mass transfer, and oxidation reaction, the lattice Boltzmann method (LBM) is utilized, which offers distinct advantages in handling complex pore geometries, multi-physics coupling, and reactive transport at the pore scale. The present model integrates, for the first time in a pore-scale LB framework, airflow driven by thermal buoyancy, convective heat and mass transfer, and Arrhenius-type oxidation kinetics within a realistic coal pile geometry. After the numerical method is validated, the effects of inflowing air velocity, inflowing air temperature, oxygen concentration, and coal particle size are discussed. With an increase in inflowing air velocity, convective heat transfer is enhanced, and the coal pile maximum temperature decreases monotonically. According to the Arrhenius equation, with an increase in the inflowing air temperature and oxygen concentration, the oxidation reaction is accelerated, and the coal pile maximum temperature increases. When the size of the coal particle increases, the oxidation reactive area decreases, and the coal pile maximum temperature decreases, while the steady temperature is not affected.

Keywords: pore-scale; coal pile; spontaneous combustion; lattice Boltzmann method

Check for updates

Academic Editors: Haipeng Jiang, Chuyuan Huang and Lijuan Liu

Received: 31 December 2025
Revised: 2 February 2026
Accepted: 6 February 2026
Published: 8 February 2026

Copyright: © 2026 by the authors. Licensee MDPI, Basel, Switzerland. This article is an open access article distributed under the terms and conditions of the Creative Commons Attribution (CC BY) license.

1. Introduction

The spontaneous combustion of coal piles threatens the safety of coal production and transportation, which is attracting more and more attention [1–4]. The spontaneous combustion of coal piles is complex, involving airflow, heat–mass transfer, and oxidation reaction. Through the oxidation reaction, heat is generated and accumulated; once the coal pile maximum temperature exceeds the critical combustion temperature, intensive spontaneous combustion occurs.

Numerous factors govern the propensity of coal piles toward spontaneous combustion. Key among these are the velocity and temperature of the incoming air, the ambient oxygen concentration, and the size distribution of the coal particles themselves [5–8]. To determine the occurrence conditions of the spontaneous combustion of coal piles, Ozdeniz

et al. formed industry-scale coal piles composed of 12 to 18 mm coal particles and measured the air velocity and air temperature continuously [5]. To deal with the spontaneous combustion of coal piles, Fierro et al. carried out physical experiments with five test coal piles and determined the heat loss coefficients [6]. Through physical experiments, different factors affecting the spontaneous combustion of coal piles are discussed. However, physical experiments are insufficient for understanding the underlying mechanisms of spontaneous combustion in coal piles. With the development of computational theories and methods, the underlying mechanisms of the spontaneous combustion of coal piles are understood numerically [9–12]. To understand the influence of oxygen concentration, Zhang et al. analyzed the coal exothermic reaction process under different oxygen concentrations and carried out the kinetic calculation of the fitting results [9]. Yuan et al. studied the effect of ventilation and determined the critical ambient temperature, namely, the minimum temperature for a coal pile to achieve thermal runaway [10]. Ejlali et al. recognized the shortcomings of some advanced models of airflow and moisture transport within and around coal piles and used a local thermal non-equilibrium approach, then compared the numerical results with the experimental data [11]. Moghtaderi et al. studied the spontaneous combustion characteristics of typical coal piles and calculated the heat and mass transfer processes [12].

To describe a coal pile, there are two typical perspectives. One is the representative volume element (RVE) scale, and the other is the pore scale. The RVE scale is suitable to describe the macroscopic physical phenomena of the spontaneous combustion of a coal pile, while the details of airflow, heat–mass transfer, and oxidation reaction are invisible. Zhao et al. proposed an oxygen consumption rate integral and compared the results at the RVE scale and at the pore scale comprehensively [13]. Wu et al. investigated the hydraulic–thermal behavior with a computational fluid dynamics model and reported that the pore scale was advantageous for complex geometries compared with the RVE scale [14]. In contrast to previous macroscopic (RVE-scale) models and existing LB applications focused on single or dual physics, the primary innovation of this work lies in the development of a comprehensive pore-scale lattice Boltzmann framework that fully couples airflow, heat transfer, mass transfer (oxygen diffusion), and exothermic oxidation reaction with thermal buoyancy effects under realistic coal pile geometries. This represents, to our knowledge, the first pore-scale LB study to integrate Arrhenius-type reaction kinetics with natural convection driven by non-uniform heating in a porous coal matrix. The model is specifically tailored to unravel the intertwined multi-physics mechanisms governing spontaneous combustion, providing insights unattainable by continuum-based approaches. Therefore, pore-scale investigation becomes indispensable for elucidating the fundamental mechanisms driving spontaneous combustion in coal piles. The spontaneous combustion of coal piles is complex, involving airflow, heat–mass transfer, and oxidation reaction. In contrast to prior macroscopic or single-physics LB models, this work presents a fully coupled pore-scale LB framework for spontaneous combustion of coal piles, incorporating airflow with buoyancy, heat transfer, oxygen diffusion, and exothermic reaction kinetics. Firstly, a pore-scale model of the spontaneous combustion of coal piles is described, and the governing equations are introduced. Next, to understand the interaction between airflow, heat–mass transfer, and oxidation reaction, the lattice Boltzmann method is utilized, which is advantageous for treating multi-field coupling compared with traditional numerical methods. Then, to prove the effectiveness of the present numerical method, method validation is conducted. Lastly, the effects of inflowing air velocity, inflowing air temperature, oxygen concentration, and coal particle size are discussed.

2. Materials and Methods

2.1. Model Description

The spontaneous combustion of coal piles is complex, involving airflow, heat/mass transfer, and oxidation reaction. Figure 1 shows the competition between airflow, heat–mass transfer, and oxidation reaction. Due to the non-uniform distribution of temperature, the temperature field affects airflow through thermal buoyancy. Conversely, airflow affects the temperature field via convective heat transfer. Meanwhile, airflow affects the concentration field via convective mass transfer. Besides airflow, the concentration field is affected by the oxidation reaction through oxygen consumption.

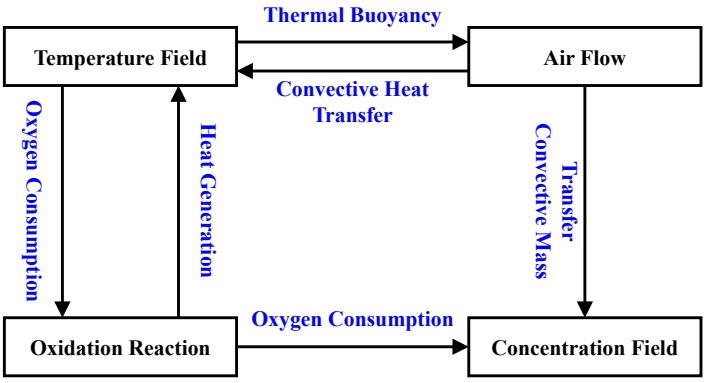


Figure 1. Interaction between airflow, heat–mass transfer, and oxidation reaction.

Affected by airflow, heat/mass transfer, and oxidation reaction, the spontaneous combustion of coal piles is complex. To understand the interaction between airflow, heat–mass transfer, and oxidation reaction, we conducted pore-scale coal spontaneous combustion research. Figure 2 shows a pore-scale model of the spontaneous combustion of a coal pile. The air flows through the coal pile from the inlet to the outlet; due to the oxidation reaction, heat accumulates and oxygen is utilized. This affects the temperature and concentration fields, which are closely related to the spontaneous combustion of coal piles. Coal particles are assumed to be circular, with radius r. The dimensionless temperature of a coal particle is set to T_1, which is affected by the oxidation reaction. The left boundary is set to fixed velocity (u_0), temperature (T_0), and oxygen concentration (C_0), while the right boundary is set to a constant pressure condition. Coal particles are modeled as circular obstacles with no-slip velocity boundary conditions, constant temperature T_1 at the particle surface, and zero oxygen flux (impermeable to oxygen).

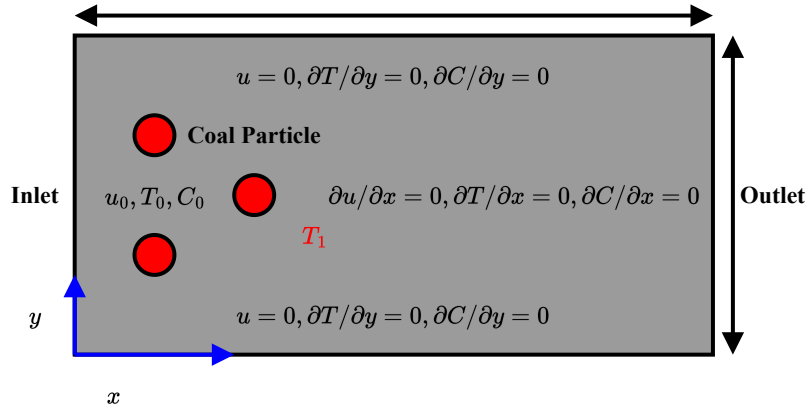


Figure 2. Pore -scale model of the spontaneous combustion of a coal pile.

To describe the spontaneous combustion of a coal pile mathematically, the governing equations are

$$\nabla \cdot \boldsymbol{u} = 0 \tag{1}$$

$$\frac{\partial \boldsymbol{u}}{\partial t} + \nabla \cdot (\boldsymbol{u} \times \boldsymbol{u}) = -\nabla p + \nu \nabla^2 \boldsymbol{u} + \boldsymbol{F} \tag{2}$$

$$\frac{\partial T}{\partial t} + \nabla \cdot (\boldsymbol{u} T) = \alpha \nabla^2 T \tag{3}$$

$$\frac{\partial C}{\partial t} + \nabla \cdot (\boldsymbol{u} C) = \beta \nabla^2 C \tag{4}$$

where $\boldsymbol{u}$ is the inflowing air velocity, T is the inflowing air temperature, C is the oxygen concentration, $\boldsymbol{F}$ is the thermal buoyancy due to a non-uniform temperature distribution, ν is the air viscosity, α is the temperature diffusivity, and β is the concentration diffusivity.

To conduct pore-scale research, dimensionless numbers are defined, namely,

$$\mathrm{Pr} = \frac{\nu}{\alpha} = 0.71 \tag{5}$$

$$\mathrm{Ra} = \frac{\gamma g L^3 \Delta T}{\nu \alpha} \tag{6}$$

where Pr is the Prandtl number, describing the relative strength between velocity diffusion and energy diffusion; Ra is the Rayleigh number, describing the effect of thermal buoyancy; ν is the air viscosity; α is the temperature diffusivity; γ is the thermal expansion coefficient; g is the gravity constant; L is the characteristic length; and ΔT is the dimensionless temperature difference. Pr = 0.71 corresponds to the Prandtl number of air at standard conditions, a common assumption in similar studies of convective heat transfer in porous media involving air.

During the spontaneous combustion of a coal pile, the oxidation reaction affects the temperature and concentration fields directly. To conveniently represent the oxidation reaction, the Arrhenius equation is adopted [15,16], namely,

$$k = AC \exp\left(-\frac{E}{RT}\right) \tag{7}$$

where k is the reaction rate, A is the pre-exponential factor, C is the oxygen concentration, E is the activation energy, R is the universal gas constant, and T is the absolute temperature. With an increase in inflowing air temperature and oxygen concentration, the oxidation reaction rate is accelerated. The Arrhenius parameters are chosen based on typical ranges reported in experimental studies of coal oxidation kinetics and are consistent with values used in prior modeling works to ensure comparability. The specific values used are representative of a generic bituminous coal.

The spontaneous combustion of coal piles is affected by numerous factors, including inflowing air velocity, inflowing air temperature, oxygen concentration, coal particle size, coal pile humidity, and solar radiation. To conduct pore-scale research, coal pile humidity and solar radiation are assumed to be constant. Meanwhile, component differences among coal particles are ignored.

2.2. Lattice Boltzmann Method

To conduct pore-scale research on the spontaneous combustion of coal piles, the lattice Boltzmann method is utilized. Compared with traditional numerical methods, the lattice Boltzmann method is advantageous [17–22]. Firstly, the spontaneous combustion of coal piles is complex, involving airflow, heat–mass transfer, and oxidation reaction. Rather than simply solving the physical equations, the lattice Boltzmann method traces the evolution of

microscopic distribution functions, which is advantageous for treating multi-field coupling compared with traditional numerical methods. Meanwhile, to conduct pore-scale research, the boundary treatment is critical. Generally, the geometric shape of coal particles is irregular, and the arrangement of coal particles is non-uniform, making the boundary treatment challenging. Due to the microscopic properties of the distribution functions, using the lattice Boltzmann model to treat complex boundaries is more convenient than traditional numerical methods. Therefore, the lattice Boltzmann method is utilized to conduct pore-scale research on the spontaneous combustion of coal piles.

To couple airflow and heat–mass transfer, the multi-distribution-function lattice Boltzmann model is adopted, and the evolution equations of the distribution functions are

$$f_i(\boldsymbol{x} + \boldsymbol{c}_i\delta t, t + \delta t) = f_i(\boldsymbol{x}, t) - \frac{1}{\tau_f}(f_i - f_i^*) + \delta t F_i \tag{8}$$

$$g_i(\boldsymbol{x} + \boldsymbol{c}_i\delta t, t + \delta t) = g_i(\boldsymbol{x}, t) - \frac{1}{\tau_g}(g_i - g_i^*) \tag{9}$$

$$h_i(\boldsymbol{x} + \boldsymbol{c}_i\delta t, t + \delta t) = h_i(\boldsymbol{x}, t) - \frac{1}{\tau_h}(h_i - h_i^*) \tag{10}$$

where $f_i(\boldsymbol{x}, t)$ is the distribution function representing airflow; $g_i(\boldsymbol{x}, t)$ is the distribution function representing heat transfer between the air and a coal particle; $h_i(\boldsymbol{x}, t)$ is the distribution function representing the mass transfer between the air and a coal particle; f_i^*, g_i^*, and h_i^* are the corresponding distribution functions at the equilibrium state; τ_f, τ_g, and τ_h are the corresponding dimensionless relaxation times; and F_i is the discrete forcing term. The D2Q9 model is utilized, where the number of dimensions is 2 and the discrete velocity is 9, and the distribution functions in the equilibrium state are

$$f_i^*(\rho, \boldsymbol{u}) = \omega_i \rho \left[1 + \frac{\boldsymbol{c}_i \cdot \boldsymbol{u}}{c_s^2} + \frac{(\boldsymbol{c}_i \cdot \boldsymbol{u})^2}{2c_s^4} - \frac{\boldsymbol{u} \cdot \boldsymbol{u}}{2c_s^2}\right] \tag{11}$$

$$g_i^*(T, \boldsymbol{u}) = \omega_i T \left[1 + \frac{\boldsymbol{c}_i \cdot \boldsymbol{u}}{c_s^2} + \frac{(\boldsymbol{c}_i \cdot \boldsymbol{u})^2}{2c_s^4} - \frac{\boldsymbol{u} \cdot \boldsymbol{u}}{2c_s^2}\right] \tag{12}$$

$$h_i^*(C, \boldsymbol{u}) = \omega_i C \left[1 + \frac{\boldsymbol{c}_i \cdot \boldsymbol{u}}{c_s^2} + \frac{(\boldsymbol{c}_i \cdot \boldsymbol{u})^2}{2c_s^4} - \frac{\boldsymbol{u} \cdot \boldsymbol{u}}{2c_s^2}\right] \tag{13}$$

where

$$\omega_i = \begin{cases} 4/9, & i = 0 \\ 1/9, & i = 1, 2, 3, 4 \\ 1/36, & i = 5, 6, 7, 8 \end{cases} \tag{14}$$

is the weight coefficient of the D2Q9 model.

To reflect the effect of thermal buoyancy, the Boussinesq assumption is adopted [23,24], namely,

$$\rho = \rho_0[1 - \gamma(T - T_0)] \tag{15}$$

where ρ_0 is the air density at temperature T_0, and γ is the expansion coefficient due to the thermal effect. The unit air gravity is

$$\boldsymbol{G} = \rho \boldsymbol{g} = \rho_0[1 - \gamma(T - T_0)]\boldsymbol{g} = \rho_0 \boldsymbol{g} - \rho_0 \gamma (T - T_0)\boldsymbol{g} \tag{16}$$

where $\rho_0 \boldsymbol{g}$ is the unit air gravity at the temperature T_0, while

$$\boldsymbol{F} = -\rho_0 \gamma (T - T_0)\boldsymbol{g} \tag{17}$$

is the thermal buoyancy due to a non-uniform temperature distribution. To add thermal buoyancy to the evolution equations of the distribution functions, the discrete thermal buoyancy is

$$F_i = \omega_i \left(\frac{\boldsymbol{c}_i - \boldsymbol{u}}{c_s^2} + \frac{\boldsymbol{c}_i \cdot \boldsymbol{u}}{c_s^4} \boldsymbol{c}_i \right) \cdot \boldsymbol{F} \tag{18}$$

In the lattice Boltzmann method, the evolution of the microscopic distribution functions is traced, and the macroscopic physical quantities are constructed by

$$\rho = \sum_i f_i \tag{19}$$

$$\boldsymbol{u} = \frac{1}{\rho} \left(\sum_i \boldsymbol{c}_i f_i + \frac{\delta t}{2} \boldsymbol{F} \right) \tag{20}$$

$$T = \sum_i g_i \tag{21}$$

$$C = \sum_i h_i \tag{22}$$

where ρ is the air density, $\boldsymbol{u}$ is the air velocity, T is the air temperature, and C is the oxygen concentration. Meanwhile, the macroscopic physical properties are determined by the dimensionless relaxation times, namely,

$$\nu = c_s^2 (\tau_f - 0.5) \delta t \tag{23}$$

$$\alpha = c_s^2 (\tau_g - 0.5) \delta t \tag{24}$$

$$\beta = c_s^2 (\tau_h - 0.5) \delta t \tag{25}$$

where ν is the kinematic viscosity, α is the temperature diffusivity, β is the concentration diffusivity, c_s is the sound speed of the D2Q9 model, and δt is the time step.

2.3. Method Validation

To validate the numerical method, a cold coal particle settling in a vertical channel is reproduced [25–30]. The particle diameter is $D = 25\delta x$, and the vertical channel has the size $W = 4D$ and $H = 320D$, where δx is the lattice spacing. The density of the particle is slightly higher than the fluid, namely, the density ratio is set to $\rho_r = 1.0023$, and the steady Reynolds number $\mathrm{Re} = DU/\nu$ is set to 40.5, where $U = \sqrt{\pi(D/2)(\rho_r - 1)g}$ is the reference settling velocity and g is the gravitational acceleration. The particle is cold, with a temperature set to $T_1 = 0$, while the fluid is hot, with a temperature set to $T_0 = 1$. The density ratio and Reynolds number are selected to match the benchmark studies for direct comparison, ensuring that the validation is consistent with the established literature. For the validation benchmark, temperatures are normalized. The fluid temperature is set to $T_0 = 1$ (reference hot state) and the particle temperature to $T_1 = 0$ (reference cold state), defining the dimensionless temperature difference $\Delta T = T_0 - T_1 = 1$.

It is reported that the motion of the particle is divided into four stages with an increase in Gr, namely, settling along the centerline, oscillating along the centerline, settling offset from the centerline, and settling along the centerline, where $\mathrm{Gr} = \gamma g D^3 \Delta T / \nu^2$ is the Grashof number, $\Delta T = T_0 - T_1$ is the temperature difference between the fluid and particle, and ν is the kinematic viscosity. Table 1 lists the equilibrium positions of a particle when Gr = 1000 and 2000. It is reported that the particle is settling offset from the centerline of the vertical channel when Gr is in the range [1000, 2000]; the present research is consistent with the previous studies. Quantitatively, the equilibrium positions of the particle are close to those described in the previous studies, proving the effectiveness of the present numerical

method. The successful reproduction of the particle's equilibrium positions under the influence of combined forced and thermal convection validates the present LB model's accuracy in handling fluid–solid interaction, momentum–thermal coupling (via Boussinesq buoyancy), and complex moving boundaries. These capabilities are directly transferable and essential for simulating the pore-scale problem of spontaneous combustion of coal piles, where airflow around irregular coal particles, buoyancy-driven flow due to non-uniform heating, and conjugate heat/mass transfer between solid and fluid phases are all critical phenomena. Therefore, this validation substantiates the model's suitability for subsequent multi-physics simulations.

Table 1. Equilibrium positions of a particle when Gr = 1000 and 2000.

Gr	Present	Yang et al. [25]	Kang et al. [27]	Yu et al. [29]
1000	2.91	2.89	2.90	2.89
2000	2.76	2.74	2.73	2.79

3. Results

The spontaneous combustion of coal piles is complex, affected by airflow, heat–mass transfer, and oxidation reaction. To conduct pore-scale research, the effects of inflowing air velocity, inflowing air temperature, oxygen concentration, and coal particle size are investigated. In the following simulations, the physical units are normalized. The reference temperature is the ambient temperature, the reference velocity is the speed of sound, the reference concentration is the oxygen concentration in the air, and the reference length is the grid spacing. According to these reference values, the dimensionless inflowing air velocity is

$$u_0 = \frac{u_0^*}{u_s}, \tag{26}$$

the dimensionless maximum temperature is

$$T_{\max} = \frac{T_{\max}^*}{T_e}, \tag{27}$$

the dimensionless inflowing air temperature is

$$T_0 = \frac{T_0^*}{T_e}, \tag{28}$$

and the dimensionless oxygen concentration is

$$C_0 = \frac{C_0^*}{C_a}, \tag{29}$$

where u_0^* is the actual inflowing air velocity, $T_{\max}^*$ is the actual maximum temperature, T_0^* is the actual inflowing air temperature, C_0^* is the actual oxygen concentration, u_s is the speed of sound, T_e is the ambient temperature, C_a is the oxygen concentration of the air.

3.1. Inflowing Air Velocity

Firstly, the effect of the inflowing air velocity is investigated. To conduct pore-scale research, the width and height of the computational domain are set to $W = 256\delta x$ and $H = 128\delta x$, respectively, and the dimensionless temperature of a coal particle is set to $T_1 = 0.5$. To understand the effect of inflowing air velocity, the inflowing air temperature is set to $T_0 = 1$, and the oxygen concentration is set to $C_0 = 1$. Figure 3 shows the maximum temperature and steady temperature of a coal pile under different inflowing air

velocities. Simulation results reveal a monotonic decline in both the peak and steady-state temperatures of a coal pile with increasing inflowing air velocity. This is attributed to enhanced convective cooling, which more effectively dissipates the heat generated by oxidation before it can accumulate locally. The temperature distribution of a coal pile is determined by both airflow and oxidation reaction. When the inflowing air velocity is small, the convective heat transfer is weak; due to the oxidation reaction, heat is generated and accumulates, and the maximum temperature and steady temperature of the coal pile are high. With an increase in inflowing air velocity, convective heat transfer becomes stronger, the heat from the oxidation reaction is transported by the airflow in a timely manner, and the maximum temperature and steady temperature of the coal pile decrease monotonically. The competition between reaction heat generation and convective cooling is obvious; the monotonic decrease in temperature is due to the increasing Peclet number and its effect on the thermal boundary layer.

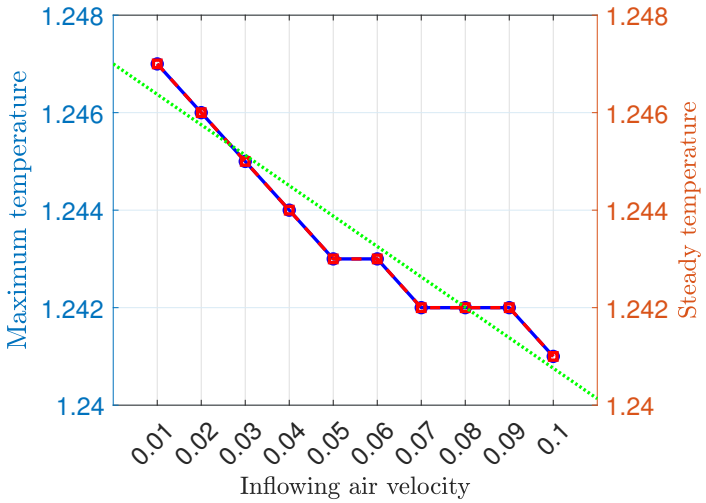
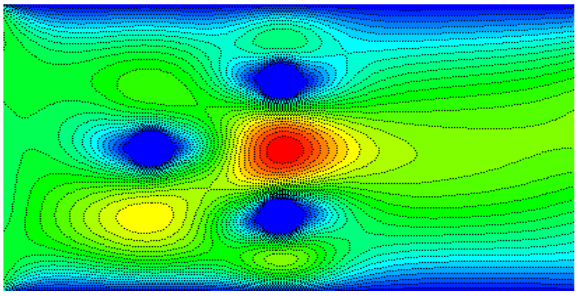


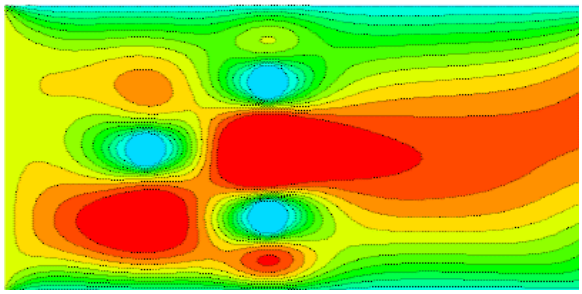
Figure 3. Maximum temperature and steady temperature of a coal pile under different inflowing air velocities.

Figure 4 shows velocity fields when the inflowing air velocities are 0.01 and 0.05. With an increase in inflowing air velocity, airflow becomes stronger. Furthermore, Figure 5 shows temperature fields when the inflowing air velocities are 0.01 and 0.05. With an increase in convective heat transfer, heat generated by the oxidation reaction is transported by the airflow in a timely manner, and the temperature distribution becomes more uniform.



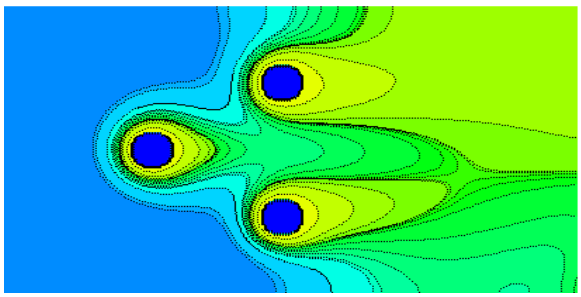
(**a**) Inflowing air velocity = 0.01.

Figure 4. *Cont.*

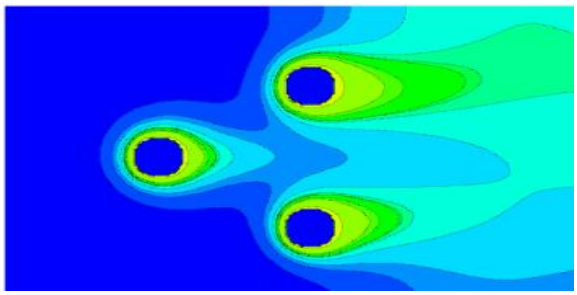


(**b**) Inflowing air velocity = 0.05.

Figure 4. Velocity fields when the inflowing air velocities are 0.01 and 0.05.



(**a**) Inflowing air velocity = 0.01.



(**b**) Inflowing air velocity = 0.05.

Figure 5. Temperature fields when the inflowing air velocities are 0.01 and 0.05.

3.2. Inflowing Air Temperature

Besides the inflowing air velocity, the spontaneous combustion of coal piles is significantly affected by the inflowing air temperature. The inflowing air temperature affects airflow and the oxidation reaction. With an increase in temperature, the rate of the oxidation reaction accelerates, and more heat is generated. To understand the effect of inflowing air temperature, the inflowing air velocity is set to $u_0 = 0.05$ and the oxygen concentration is set to $C_0 = 1$. Figure 6 shows the maximum temperature and steady temperature of a coal pile under different inflowing air temperatures. With an increase in inflowing air temperature, the maximum temperature and steady temperature of the coal pile increase. There is a critical inflowing air temperature; when the inflowing air temperature is less than 1.25, the maximum temperature increases slowly, while the maximum temperature increases rapidly when the inflowing air temperature is greater than 1.25. The temperature distribution inside a coal pile is affected by airflow and oxidation reaction. When the inflowing air temperature is low, the oxidation reaction is suppressed; therefore, the maximum temperature of the coal pile is relatively low. Once the inflowing air temperature exceeds the critical temperature, the oxidation reaction accelerates significantly and becomes dominant over the convective heat transfer, and the maximum temperature increases rapidly. Due to the nonlinear, exponential nature of the Arrhenius law, once the air temperature is beyond a critical point, a small change can lead to rapid thermal runaway.

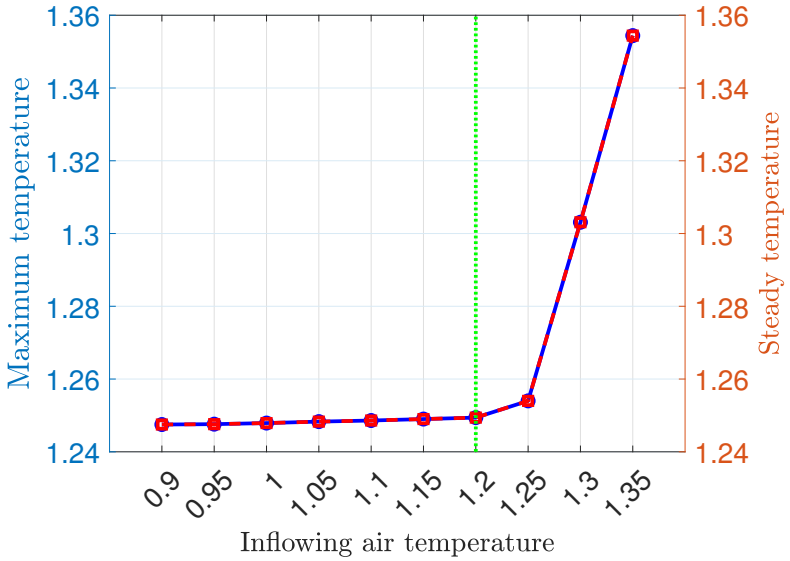
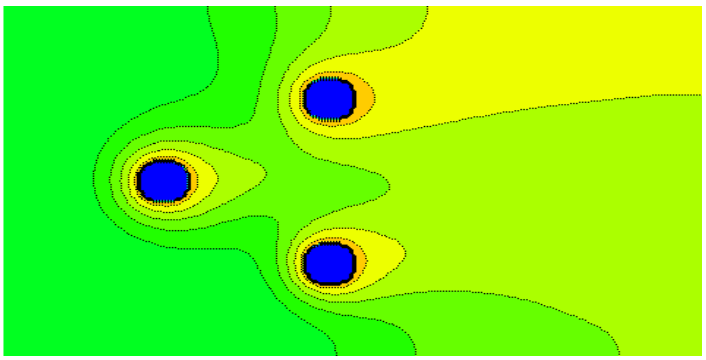
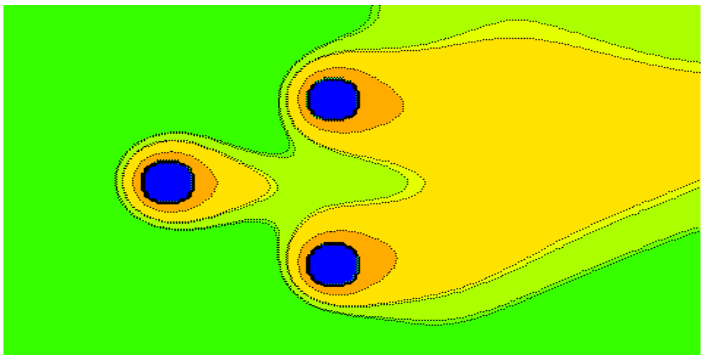


Figure 6. Maximum temperature and steady temperature of a coal pile under different inflowing air temperatures.

Furthermore, Figure 7 shows temperature fields when inflowing air temperatures are 1.1 and 1.3. With increasing inflowing air temperature, according to the Arrhenius equation, the oxidation reaction rate is accelerated. Compared with the inflowing air temperature $T_0 = 1.1$, the temperature around the coal particles is obviously higher when the inflowing air temperature is 1.3, which is related to the intensified heat generation due to the oxidation reaction.



(**a**) Inflowing air temperature=1.1.



(**b**) Inflowing air temperature=1.3.

Figure 7. Temperature fields when the inflowing air temperatures are 1.1 and 1.3.

3.3. Oxygen Concentration

By generating heat and consuming oxygen, the oxidation reaction directly affects temperature and concentration fields. Referring to the Arrhenius equation, the oxidation reaction rate is closely related to oxygen concentration. Therefore, the effect of oxygen concentration is understood. Where the inflowing air velocity is set to $u_0 = 0.05$, the inflowing air temperature is set to $T_0 = 1$. Figure 8 shows the maximum temperature and steady temperature of a coal pile under different oxygen concentrations. Similar to inflowing air temperature, there is a critical oxygen concentration: at low oxygen concentrations of less than 0.8, the oxidation reaction rate is small, close to 0; therefore, the highest temperature of a coal pile is insensitive to oxygen concentration. Once the oxygen concentration exceeds the critical concentration, reflecting the transition from diffusion-limited to reaction-limited oxidation, the oxidation reaction rate increases monotonically and heat is generated and accumulates, leading to the rapid increase in the highest temperature of a coal pile.

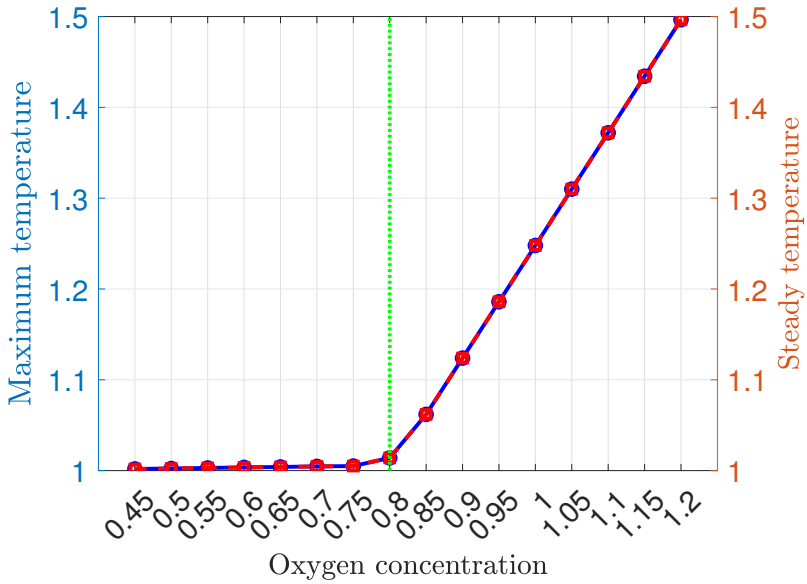


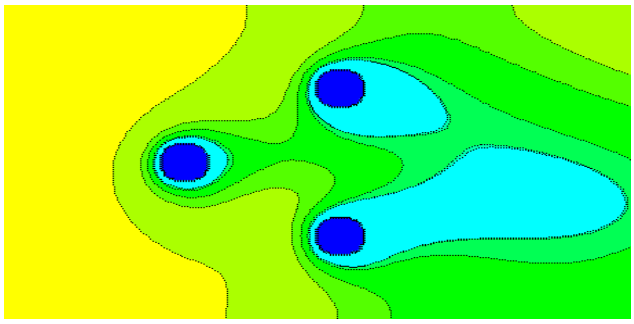
Figure 8. Maximum temperature and steady temperature of a coal pile under different oxygen concentrations.

Furthermore, Figure 9 shows the temperature fields when the oxygen concentration is 0.7 and 0.9. When oxygen concentration is low, the oxidation reaction is weak and the heat generated can be neglected; therefore, the highest temperature of a coal pile is close to the inflowing air temperature. Once the oxygen concentration exceeds the critical concentration, the oxidation reaction accelerates and heat is generated continuously; as a result, the temperature around coal particles increases rapidly.

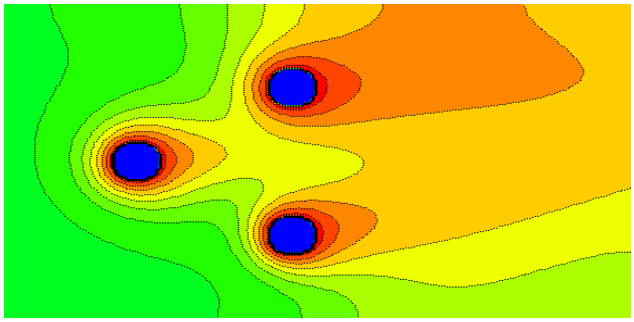
3.4. Coal Particle Size

The spontaneous combustion of coal piles is complex. Besides inflowing air velocity, inflowing air temperature, and oxygen concentration, the effect of coal particle size is investigated. To represent the influence of coal particle size, the porosity of a coal pile is set to 0.9, the inflowing air velocity is $u_0 = 0.05$, the inflowing air temperature is $T_0 = 1$, the oxygen concentration is $C_0 = 1$. Figure 10 shows the maximum temperature and steady temperature of a coal pile when coal particle sizes are different. The maximum temperature is obviously influenced by coal particle size; with an increase in coal particle size, maximum temperature decreases. When the porosity of the coal pile is the same, smaller coal particle sizes correspond to a larger oxidation reactive area and greater heat generation; therefore, the maximum temperature is higher. In contrast to the maximum temperature, the steady temperature is insensitive to coal particle size. For small coal particle sizes, the steady

temperature is less than the maximum temperature, while for larger coal particle sizes, the steady temperature is greater than the maximum temperature. The steady temperature of the coal pile is affected by the environmental factors, including inflowing air velocity, inflowing air temperature, and oxygen concentration. Under the same environmental factors, the steady temperature is not affected by coal particle size. The reduced particle size increases specific surface area (reactive area) while simultaneously decreasing pore throat sizes, which impedes convective cooling; this dual effect explains the strong impact on peak temperature but not on steady-state temperature.



(**a**) Oxygen concentration = 0.7.



(**b**) Oxygen concentration = 0.9.

Figure 9. Temperature fields when the oxygen concentration is 0.7 and 0.9.

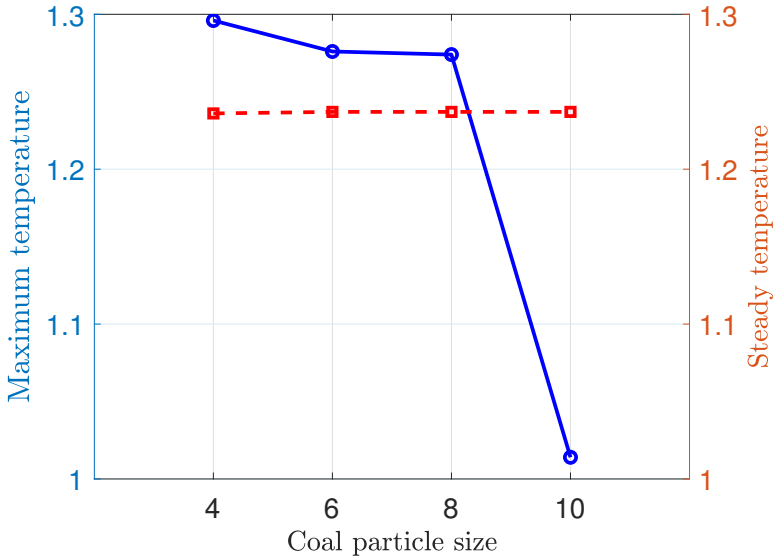
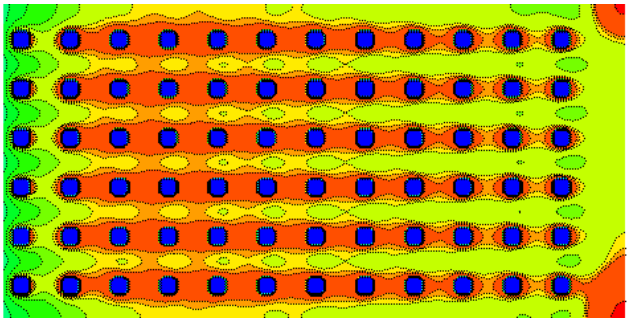
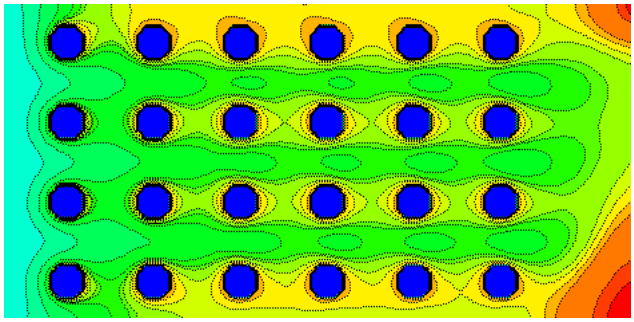


Figure 10. Maximum temperature and steady temperature of the coal pile when the coal particle sizes are different.

Figure 11 shows the temperature distribution around coal particles when coal particle sizes are different. Under the same porosity, with a decrease in coal particle size, the coal particle number increases; therefore, the oxidation reactive area increases. Meanwhile, the smaller the coal particle, the narrower the channel between the adjacent coal particles, which is not conducive to convective heat transfer; consequently, the maximum temperature is higher.



(**a**) Coal particle size = 4.



(**b**) Coal particle size = 8.

Figure 11. Temperature distribution around coal particles when coal particle sizes are different.

4. Discussion

The present model has some limitations. Firstly, to simplify the present study, coal particle composition is assumed to be constant. However, the real coal particle composition may be quite different, which affects the oxidation reaction and heat–mass transfer directly. Secondly, to save computational costs, a 2D simulation is conducted. Though the 2D result is similar to the 3D case, the 2D simplification may affect three-dimensional natural convection patterns. In the next stage, conducting a 3D simulation of coal spontaneous combustion is necessary. In addition, in the present study, we use a simplified Arrhenius kinetics model without intermediate reaction products. In fact, the oxidation reaction of coal particles is quite complex, and the intermediate reaction products can affect the oxidation process significantly. However, describing the intermediate reaction process accurately is challenging. In the future, it would be valuable to incorporate detailed reaction mechanisms to understand coal spontaneous combustion.

The aim of the present study is to establish a pore-scale modeling framework and investigate parametric trends. We agree that a comparison with experimental data significantly strengthens validation. Our key findings, including the trend of decreasing maximum temperature with increasing air velocity and the existence of a critical temperature/oxygen concentration, are consistent with qualitative or semi-quantitative trends reported in the experimental literature on coal pile self-heating [5,6,9,10]. Furthermore, to compare simulation results with experimental results, we will conduct a 3D simulation of coal spontaneous combustion. By using the same parameters, we can compare simulation

results with experimental results, which will be persuasive in proving the effectiveness of the present model.

5. Conclusions

Pore-scale research on the spontaneous combustion of coal piles utilizing the lattice Boltzmann method is conducted. The spontaneous combustion of coal piles is complex, involving airflow, heat–mass transfer, and oxidation reaction. To deepen the understanding of the spontaneous combustion of coal piles, the effects of inflowing air velocity, inflowing air temperature, oxygen concentration, and coal particle size are investigated, and the following conclusions are drawn:

(1) Pore-scale analysis confirms that higher inflowing air velocities intensify convective heat transfer, leading to a significant reduction in the equilibrium temperature of a coal pile, thereby mitigating the risk of thermal runaway.

(2) The effect of inflowing air temperature is significant: with an increase in inflowing air temperature, the oxidation reaction rate accelerates and the maximum temperature and steady temperature of the coal pile increase.

(3) There is a critical oxygen concentration. When the oxygen concentration is low, the oxidation reaction is suppressed, but once the oxygen concentration exceeds the critical concentration, the oxidation reaction accelerates and the maximum temperature and steady temperature increase.

(4) Under the same environmental factors, the smaller the coal particle size, the greater the oxidation reactive area and the higher the maximum temperature of the coal pile.

By conducting pore-scale research, the underlying mechanisms of the spontaneous combustion of coal piles are explored, which is helpful in improving the safety of coal production and transportation. Through the present study, the findings suggest that controlling inlet airflow and monitoring oxygen concentration near critical thresholds can mitigate spontaneous combustion. Smaller coal particles require closer thermal monitoring due to higher peak temperatures.

Author Contributions: Y.W., Writing—Original Draft; M.Z., Formal Analysis; X.W., Investigation; D.Z., Conceptualization; K.L., Resources; S.X., Resources; J.H., Methodology. All authors have read and agreed to the published version of the manuscript.

Funding: The research was supported by the National Natural Science Foundation of China (52376133, 52574280 and 51904281) and an Open Research Grant of the Joint National–Local Engineering Research Center for Safe and Precise Coal Mining (EC2022002), and their support is also gratefully acknowledged.

Data Availability Statement: The original contributions presented in this study are included in the article. Further inquiries can be directed to the corresponding author.

Conflicts of Interest: The authors declare no conflicts of interest.

References

1. Onifade, M.; Genc, B. A review of research on spontaneous combustion of coal. *Int. J. Min. Sci. Technol.* **2020**, *30*, 303. [CrossRef]
2. Liang, Y.; Zhang, J.; Wang, L. Forecasting spontaneous combustion of coal in underground coal mines by index gases: A review. *J. Loss Prev. Process Ind.* **2019**, 57, 208. [CrossRef]
3. Onifade, M.; Genc, B. Spontaneous combustion of coals and coal-shales. *Int. J. Min. Sci. Technol.* **2018**, *28*, 933. [CrossRef]
4. Liu, W.; Qin, Y. Multi-physics coupling model of coal spontaneous combustion in longwall gob area based on moving coordinates. *Fuel* **2017**, *188*, 553. [CrossRef]
5. Ozdeniz, A. Determination of Spontaneous Combustion in Industrial-scale Coal Stockpiles. *Energy Sources* **2010**, *32*, 665. [CrossRef]
6. Fierro, V.; Miranda, J.; Romero, C. Prevention of spontaneous combustion in coal stockpiles: Experimental results in coal storage yard. *Fuel Process. Technol.* **1999**, *59*, 23. [CrossRef]

7. Chen, X.; Stott, J. Oxidation rates of coals as measured from one-dimensional spontaneous heating. *Combust. Flame* **1997**, *109*, 578. [CrossRef]
8. Anghelescu, L.; Diaconu, B. Advances in Detection and Monitoring of Coal Spontaneous Combustion: Techniques, Challenges, and Future Directions. *Fire* **2024**, *7*, 354. [CrossRef]
9. Zhang, Y.; Zhang, Y.; Li, Y. Heat effects and kinetics of coal spontaneous combustion at various oxygen contents. *Energy* **2021**, *234*, 121299. [CrossRef]
10. Yuan, L.; Smith, A. The effect of ventilation on spontaneous heating of coal. *J. Loss Prev. Process Ind.* **2012**, *25*, 131. [CrossRef]
11. Ejlali, A.; Mee, D.; Hooman, K. Numerical modelling of the self-heating process of a wet porous medium. *Int. J. Heat Mass Transf.* **2011**, *54*, 5200. [CrossRef]
12. Moghtaderi, B.; Dlugogorski, B.; Kennedy, E. Effects of Wind Flow on Self-Heating Characteristics of Coal Stockpiles. *Process Saf. Environ. Prot.* **2000**, *78*, 445. [CrossRef]
13. Zhao, X.; Dai, G.; Qin, R. Spontaneous combustion characteristics of coal based on the oxygen consumption rate integral. *Energy* **2024**, *288*, 129626. [CrossRef]
14. Wu, C.; Ferng, Y.; Chieng, C. Investigating the advantages and disadvantages of realistic approach and porous approach for closely packed pebbles in CFD simulation. *Nucl. Eng. Des.* **2010**, *240*, 1151. [CrossRef]
15. Chung, Y.; Green, W. New modified Arrhenius equation to describe the temperature dependence of liquid phase reaction rates. *Chem. Eng. J.* **2025**, *516*, 163300. [CrossRef]
16. Shree, R.; Mallikarjun, B.; Basma, S. Application of fibonacci wavelet frame operational matrix for the analysis of arrhenius-controlled heat transportation flow in a microchannel. *Case Stud. Therm. Eng.* **2024**, *63*, 105326. [CrossRef]
17. David, W.; Josef, W.; Steffen, S. A quantum algorithm for the lattice-Boltzmann method advection-diffusion equation. *Comput. Phys. Commun.* **2025**, *306*, 109373.
18. Chai, Z.; Huang, C.; Shi, B. A comparative study on the lattice Boltzmann models for predicting effective diffusivity of porous media. *Int. J. Heat Mass Transf.* **2016**, *98*, 687. [CrossRef]
19. Marco, L.; Adriano, T.; Sauro, S. Thread-safe multiphase lattice Boltzmann model for droplet and bubble dynamics at high density and viscosity contrasts. *Phys. Fluids* **2025**, *37*, 072111. [CrossRef]
20. Huang, R.; Wu, H. A modified multiple-relaxation-time lattice Boltzmann model for convection–diffusion equation. *J. Comput. Phys.* **2014**, *274*, 50. [CrossRef]
21. Mohammad, A.; Spencer, S.; Zahra, K. A multi-domain lattice Boltzmann mesh refinement method for non-Newtonian blood flow modeling. *Phys. Fluids* **2025**, *37*, 013107.
22. Mohamad, A.; Kuzmin, A. A critical evaluation of force term in lattice Boltzmann method, natural convection problem. *Int. J. Heat Mass Transf.* **2010**, *53*, 990. [CrossRef]
23. Hu, J.; Xu, M.; Zhang, J. A consistent treatment of moving boundaries with thermal convection for lattice Boltzmann method. *Phys. Fluids* **2021**, *33*, 123312. [CrossRef]
24. Hu, J.; Guo, Z. A numerical study on the migration of a neutrally buoyant particle in a Poiseuille flow with thermal convection. *Int. J. Heat Mass Transf.* **2017**, *108*, 2158. [CrossRef]
25. Yang, B.; Chen, S.; Cao, C. Lattice Boltzmann simulation of two cold particles settling in Newtonian fluid with thermal convection. *Int. J. Heat Mass Transf.* **2016**, *93*, 477. [CrossRef]
26. Eshghinejadfard, A.; Thevenin, D. Numerical simulation of heat transportation in particulate flows using a thermal immersed boundary lattice Boltzmann method. *Int. J. Heat Fluid Flow* **2016**, *60*, 31. [CrossRef]
27. Kang, S.; Hassan, Y. A direct-forcing immersed boundary method for the thermal lattice Boltzmann method. *Comput. Fluids*, **2011**, *49*, 36. [CrossRef]
28. Feng, Z.; Michaelides, E. heat transportation in particulate flows with Direct Numerical Simulation (DNS). *Int. J. Heat Mass Transf.* **2009**, *52*, 777. [CrossRef]
29. Yu, Z.; Shao, X.; Wachs, A. A fictitious domain method for particulate flows with heat transportation. *J. Comput. Phys.* **2006**, *217*, 424. [CrossRef]
30. Gan, H.; Chang, J.; Feng, J. Direct numerical simulation of the sedimentation of solid particles with thermal convection. *J. Fluid Mech.* **2003**, *481*, 385. [CrossRef]

Disclaimer/Publisher's Note: The statements, opinions and data contained in all publications are solely those of the individual author(s) and contributor(s) and not of MDPI and/or the editor(s). MDPI and/or the editor(s) disclaim responsibility for any injury to people or property resulting from any ideas, methods, instructions or products referred to in the content.